Mutational analysis of the Qi-site proton pathway in yeast cytochrome bc1 complex

Zehua Song, Yangfeng Hu, Bogdan I. Iorga, Cindy Vallières, Nicholas Fisher, Brigitte Meunier

Mutational analysis of the Q_i-site proton pathway in yeast cytochrome bc_1 complex

Zehua Song[a], Yangfeng Hu[a], Bogdan I. Iorga[b] Cindy Vallières[c], Nicholas Fisher[d], and Brigitte Meunier[e]

Affiliation:

a Translational Research Institute, Henan Provincial People's Hospital, School of Medicine, Henan University, Zhengzhou, China

b Université Paris-Saclay, CNRS, Institut de Chimie des Substances Naturelles, UPR 2301, 91198, Gif-sur-Yvette, France.

c School of Life Sciences, University of Nottingham, University Park, Nottingham, NG7 2RD, UK.

d MSU-DOE Plant Research Laboratory, Michigan State University, East Lansing, MI 48824, USA.

e Institute for Integrative Biology of the Cell (I2BC), CEA, CNRS, Université Paris-Saclay, 91198, Gif-sur-Yvette, France

Corresponding authors:

Brigitte Meunier Institute for Integrative Biology of the Cell (I2BC), 1 avenue de la Terrasse, 91198 Gif-sur-Yvette, France

brigitte.meunier@i2bc.paris-saclay.fr

Nicholas Fisher, MSU-DOE Plant Research Lab, 612 Wilson Road, East Lansing, MI 48824

nefisher@msu.edu

Summary

The respiratory cytochrome bc_1 complex functions as a protonmotive ubiquinol:cytochrome *c* oxidoreductase. Lysine 228 (K228) located within the quinol reduction (Q_i) site of the bc_1 complex, has been reported as a key residue for proton transfer during the redox chemistry cycle to substrate quinone at Q_i. In yeast, while single mutations had no effect, the combination of K228L and F225L resulted in a severe respiratory growth defect and inhibition of O_2 consumption in intact cells. The inhibition was overcome by uncoupling the mitochondrial membrane or by suppressor mutations in the region of K228L-F225L. We propose that the K228L mutation introduces energetic (and kinetic) barriers into normal electron- and proton transfer chemistry at Q_i, which are relieved by dissipation of the opposing protonmotive force or through the restoration of favourable intraprotein proton transfer networks via suppressor mutation.

Keywords: proton/electron transfer, respiratory complex, complex III catalytic activity, mitochondrial mutations.

Introduction

The cytochrome bc_1 complex of the mitochondrial respiratory chain catalyses the oxidation of ubiquinol and the reduction of cytochrome *c*, which is coupled to the movement of proton across the mitochondrial inner membrane.

Three subunits form the catalytic core of this multimeric enzyme: cytochrome c_1, the iron-sulfur protein and cytochrome *b*. The latest, mitochondrially encoded in all eukaryotes, is the central and largest subunit, consisting of eight transmembrane helices and providing the two ubiquinol (and inhibitor) binding sites, the quinol oxidation site (Q_o) and the quinone reduction site (Q_i).

These two sites are located on opposite sides of the membrane and linked by a transmembrane electron-transfer pathway (via hemes b_l and b_h). An ubiquinol molecule binds at the Q_o-site, is deprotonated, and transfers one electron through the iron-sulphur protein and cytochrome c_1 to cytochrome *c*, forming a semiquinone. The semiquinone then reduces b_l which in turn functions as reductant for b_h. Ferroheme b_h then reduces the ubiquinone bound at the Q_i-site, forming a stable (tightly bound) semiquinone species, with associated proton uptake from the mitochondrial matrix. A second ubiquinol oxidation at the Q_o-site completes the cycle with the formation of fully reduced ubiquinol at the Q_i-site. The oxidation and reduction of ubiquinol/ubiquinone require proton movement to and from the aqueous phase, and thus proton pathways that are not as well defined as electron transfer paths.

Residue K228 (yeast (*Saccharomyces cerevisae*) numbering) is a key residue of a pathway for the uptake of protons from the matrix into the Qi-site, first termed cardiolipin /K-pathway [1]. In this pathway, K228 would acquire a proton from the bound cardiolipin, then passes it via water molecules into the Q_i-site for the reduction of quinone. Molecular dynamics studies suggests that the sidechain of K228, once protonated, rotates into the Q_i-site to form a salt-bridge with D229 [2]. In the bacterial enzyme, replacement of both K228 and D229 by non-

protonable residues fully blocked the Q_i-site function by disabling the proton transfer path [3].

K228 is highly conserved amongst species. However in yeast, the replacement of K228 by a methionine, isoleucine or leucine is well tolerated and the enzyme is active (see for instance [4] and references within). Nearby protonatable residues H202 and /or D229 and/or water molecules might take over K228 activity and render the residue dispensable. Interestingly in the human malaria parasite *Plasmodium falciparum* and other apicomplexans, a leucine replaces K228. In addition, while H202 and D229 are conserved, other amino-acid substitutions (as compared to yeast) are found in the vicinity.

In our attempts to reconstruct the Q_i-site of yeast bc_1 complex to render the pocket more similar to the *P.falciparum* Q_i-site (and thus a potentially convenient model for the parasite enzyme), we found that residues cannot be interchanged without deleterious effect. Here, we studied the effect of *Plasmodium*-like substitutions of K228 and neighbour residues. The combination of K228L and F225L, naturally present in *P.falciparum*, caused a severe respiratory growth defect while the bc_1 complex remained apparently functional in uncoupled mitochondria. The growth defect can be overcome by suppressor mutations in the vicinity of the primary mutations.

Materials and Methods

Materials and growth media

Equine cytochrome *c*, decylubiquinone, superoxide dismutase and catalase were obtained from Sigma Aldrich. The following media were used for the growth of yeast: YPD (1% yeast extract, 2% peptone and 3% glucose), YPGal (1% yeast extract, 2% peptone and 2% galactose) and YPG (1% yeast extract, 2% peptone and 2% glycerol).

Yeast mutants

The multiple mutations were introduced in yeast cytochrome *b* by side-directed mutagenesis and mitochondrial transformation [5,6]. In all experiments, control and mutants have identical nuclear and mitochondrial genomes with the exception of the mutations introduced in the cytochrome *b* gene.

Measurement of decylubiquinol-cytochrome *c* reductase activity

Yeast mitochondria were prepared as in [7]. Concentration of bc_1 complex in the mitochondrial samples was determined from dithionite-reduced optical spectra, using ε=28.5 mM^{-1} cm^{-1} at 562 nm *minus* 575 nm.
Decylubiquinol-cytochrome *c* reductase activities were determined at room temperature by measuring the reduction of cytochrome *c* (final concentration of 20 µM) at 550 nm *versus* 540 nm over one-min time-course in 10 mM potassium phosphate pH 7, 0.01% (w/v) lauryl-maltoside and 2 mM KCN. Mitochondria were added to obtain a final concentration of 5-15 nM bc_1 complex. Activity was initiated by the addition of decylubiquinol. Each measurement was repeated three to five times and the values obtained were averaged. Activities (k_{cat}) were determined as the cytochrome *c* reduction rate per bc_1 complex.
Apparent K_M values were estimated from the plots of cytochrome *c* reduction rates *vs* decylubiquinol concentrations, as the decylubiquinol concentrations required to obtain 50% of

the observed maximum rate of cytochrome *c* reduction. In order to assess the production of superoxide (SO), cytochrome *c* reduction rates were recorded in absence and in presence of superoxide dismutase and catalase, both at 225 units/mL, in potassium phosphate buffer 50 mM pH 7 with 0.1mM KCN. The measurements were repeated at least three times and the obtained values averaged.

Aconitase and fumarase measurement using cell extracts

The aconitase and fumarase activities were determined spectrophotometrically by monitoring the formation of cis-aconitate and fumarate at 240 nm and 25°C. Briefly, cell extracts were prepared from 2.0×10^8 cells (OD_{600} ~20) grown on YPGal. Lysis was performed at 4°C in 10 mM MES buffer, pH6 containing 0.6 mM $MnCl_2$ and deprived of oxygen (by bubbling with nitrogen gas) with 0.5 mm glass beads (v/v), by vortexing for 30 s followed by incubation on ice for 30 s, repeating the process seven times. Cell debris was removed by centrifugation at 13,000 rpm for 5 min, and the resulting supernatant was aliquoted and frozen immediately in liquid nitrogen and kept at -80°C. Samples were thawed just before the assay. Protein concentration was determined spectrophotometrically with the Bio-Rad protein assay kit, according to the manufacturer's instructions.
For the aconitase activity, the assay mixture contained 50 mM potassium phosphate buffer, pH 7.4, 30 mM sodium isocitrate, 0.6 mM $MnCl_2$, and 150-250 µg of protein for a final volume of 1 ml. For the fumarase activity, the assay mixture contained 50 mM potassium phosphate buffer, pH 7.4, 50 mM L-malic acid and 150-250 µg of protein for a final volume of 1 ml. The absorbance changes were measured for 20 min, and the activity was calculated from the slope of the linear portion; ε_{240} = 3.6 mM^{-1} cm^{-1} for cis-aconitate and ε_{240} = 2.44 mM^{-1} cm^{-1} for fumarate.

Measurement of oxygen consumption by intact cells

Yeast were cultivated in YPGal medium at 28°C in flasks with vigorous agitation for a good aeration. Cells were harvested at an OD_{600} nm of 15-18. After centrifugation, the cells were resuspended in fresh YPGal to an OD_{600} nm of around 250 and immediately used for the assay. Oxygen consumption was monitored in YPGal using an oxygen electrode at 25°C before and after the addition of 15 µM CCCP (carbonyl cyanide m-chlorophenyl hydrazine). The measurements were repeated at least three times and the values averaged. The oxygen consumption activities were determined as oxygen uptake rates per OD_{600nm} cells.

Results

Plasmodium-like mutations in proton pathway of yeast bc_1 complex Q_i-site

In the region of the proton-pathway leading to the Qi-site, two residues that differ between yeast and *P.falciparum* seemed particularly interesting to study, namely residues 228 and 225. These residues are located at the entry towards the Qi-site. Analysis of the large collection of eukaryote cytochrome *b* sequence publicly available (over 8,500) showed that these two residues are conserved. K228 is present in 98.8% of the analysed sequences but it is replaced by leucine in *P.falciparum*. Position 225 is occupied by an aromatic residue in most of the organisms (phenylalanine in 68.5%, tyrosine in 27.9% or histidine in 1.7%) whereas it is also a leucine in the parasite. D229 that would connect with K228 for proton transfer [3], and

H202 and S206 possibly involved in substrate binding and protonation are conserved between yeast and *P.falciparum*.

Single mutants F225L and K228L were already available and previously studied. We produced the double mutant F225L – K228L, and a mutant, named PFQi11 that combined F225L – K228L with two other changes, namely M221F and V233F. Residue 233, (valine in yeast and phenylalanine in the parasite) is not well conserved and is not *sensu stricto* in the Q_i-site although its sidechain points towards bound antimycin. Residue 221 is a methionine in yeast while it is a phenylalanine in *P. falciparum* and in most of the organisms (97.2%). The position of the residues are shown in Fig.1

Respiratory growth competence and bc_1 complex activity

We had previously tested the effect of single mutations M221F, F225L and K228L [8]. The mutations had no or minor effect on growth competence and bc_1 complex activity. The effect of V233F alone was not tested. The mutation was unlikely to have a deleterious effect, the residue being located slightly outside the Q_i-site.

By contrast, the combination F225L and K228L caused a severe growth defect. PFQi11 that harbours F225L and K228L with M221 and V233F was also unable to grow on respiratory medium (Fig.2).

Mitochondria were then prepared from the two mutants and the bc_1 complex activity was monitored. Surprisingly, PFQi11 showed a WT bc_1 complex activity and the double mutant presented only a two-fold decreased activity which could not account for the complete respiratory growth defect (Table 1).

K_M for decylubiquinol were estimated as described in Materials and Methods. PFQi11, the double mutant F225L- K228L, and the single mutant K228L showed a slightly higher K_M of 7-8 μM. K_M for F225L was as WT. The slight difference in K_M values did not suggest severe alterations in the binding environment or the accessibility of the quinol/quinone into the site.

We then checked whether the apparent high rate of cytochrome *c* reduction observed in PFQi11 and the double mutant F225L- K228L might be due to SO over-production by the bc_1 complex during the assay. We thus monitored SO production as the superoxide dismutase-sensitive rate of cytochrome *c* reduction (Materials and Methods). The difference between the reduction rate in the absence and the presence of added superoxide dismutase gives the contribution of the cytochrome *c* reduction by SO to the overall cytochrome *c* reductase activity. No SO production was detected (not shown), in contrast to the observed SO overproduction caused by *Plasmodium*-like mutations in the Q_o-site [9] Thus there was no indication of a severe Q-cycle dysfunction in the PFQi11 and F225L- K228L bc_1 complex, in the conditions of the assays, explaining the respiratory growth defect.

Suppressor mutations

We then investigated ways to overcome the growth defect. Starting with PFQi11, we selected colonies with restored respiratory growth. To that end, several subclones of the mutant were incubated on YPG medium. After two to four weeks, respiratory competent colonies appeared. Eight independent colonies (each from different subclones) were analysed. The

suppressor mutations, identified by sequencing the cytochrome *b* gene were T232I (found in four colonies); N31D, Y28S, K228M and the reversion back to WT of residue F225 (observed once). The location of the primary mutations and suppressors is shown in Fig.1.

The residue at position 28 is not strongly conserved amongst organisms, although it is mostly a tyrosine or a phenylalanine in fungi and protists, but a serine is found in 15% of animal cytochrome *b*. N31 is well conserved as it is found in 94.7% of the analysed sequences. An aspartate was not reported at that position. At position 232, a glycine is found in 90.1% of the sequences but it is a threonine in most of the fungi. In protists, the position is occupied by glycine, alanine or serine. An isoleucine was not reported. Thus the secondary mutations introduced original residues in that region of the Qi-site that resulted in a restored function.

The respiratory growth competence and bc_1 complex activities of the suppressors were assessed (Fig.2 and Table 1). The secondary mutations restored a good growth. The bc_1 complex activities varied from a two-fold decreased activity as compared to WT (27 s^{-1} SUP2) to WT level (SUP1 and SUP6). The K_M for quinol was decreased (3 to 5 μM) and thus closer or identical to WT. None of the suppressors showed SO overproduction in the bc_1 complex assay (not shown).

Oxygen consumption of cells

In order to obtain more information on the cause of the growth defect in PFQi11 and F225L-K228L, we monitored the oxygen consumption activity of freshly grown WT and mutant cells.

PFQi11 and F225L-K228L displayed low oxygen consumption activities under physiological conditions (without added uncoupler): 30% and 7% of the WT rate, respectively (Fig.3A), which clearly reflects the respiratory growth deficiency. Upon CCCP addition (Fig.3B), a ten-fold increase in oxygen consumption rate was observed in the mutant cells, compared to the three-fold increase observed with WT cells. Thus in presence of CCCP, PFQi11 oxygen consumption reached WT level. F225L-K228L rate remained lower (28% of WT rate). The single mutation F225L and K228L had no or much milder effect and their behaviour was closer to that of the WT.

The oxygen consumption activities of the suppressors were also tested. As showed in Fig. 3, the suppressor mutations restored normal oxygen consumption activity and reactivity to CCCP.

These data suggested that in PFQi11, the bc_1 complex activity, and by consequent the respiratory chain, were blocked under normal physiological conditions, i.e. in untreated cells with coupled mitochondria. Addition of CCCP released that inhibition as the O_2 consumption activity in CCCP treated cells reached WT rate.

It should be noted that PFQi11 bc_1 complex activities found to reach WT level (Table 1) were assayed in buffer without osmotic protection and with detergent, thus on broken uncoupled mitochondrial membranes.

The double mutant F225L-K228L displayed the same behaviour as PFQi11 but with a more severe defect. Thus the two additional changes, M221F and V233F, seem to attenuate the deleterious effect of F225L-K228L.

Effect of PFQi11 mutations on ROS production in cells

In the mutant cells (with intact mitochondria), the Q_i-site mutations could slow the reduction of quinone, resulting in electron accumulation on heme b_l. This could subsequently result in ROS generation from Q_o-bound semiquinone, similarly to the antimycin-inhibited state (see for instance [10] and references within). We thus investigated whether ROS were over-produced in PFQi11 and F225L- K228L cells as a result of inhibited bc_1 complex.

We measured the activity of aconitase, a tricarboxylic acid (TCA) cycle, located in the mitochondrial matrix and known to be highly sensitive to ROS damage. As a control, the activity of the TCA enzyme fumarate that is not sensitive to oxidative attack was monitored in parallel. As shown in Fig.4, the aconitase activity was over two-fold decreased in the mutants, clearly indicating an increased ROS level.

As mentioned above, SO production was not observed in the bc_1 complex assays, which was performed on broken uncoupled mitochondria.

The data argue for a dysfunction of the bc_1 complex in cells.

The increased oxidative stress in the mutants could also be due to ROS production by the NADH- and succinate-dehydrogenases. The bc_1 complex activity being inhibited in the mutant cells, electrons are expected to accumulate on the redox centres of upstream respiratory enzymes, with possible subsequent leak to oxygen.

Discussion

The combination of the Q_i-site mutations K228L and F225L resulted in a blocked O_2 consumption in intact cells (i.e. with intact coupled mitochondria). The inhibition was released 1) upon addition of the uncoupler CCCP that collapsed the transmembrane protonmotive force and in broken uncoupled mitochondria; 2) by suppressor mutations in the vicinity of F255L-K228L.

We hypothesize that proton entry into the Q_i-site would be hindered by the double mutation, which would slow down the electron transfer- and quinone reduction chemistry at the Q_i-site. This is not the limiting step of the overall reaction catalysed by the bc_1 complex (which is the first electron transfer reaction at the Q_o-site [11]). This offers an explanation for the WT rate of cytochrome *c* reduction observed in the assays with broken mitochondria prepared from PFQi11 (Table 1). In intact cells with coupled mitochondria however, the thermodynamic backpressure of the membrane potential would be expected to further retard proton entry and (electrogenic) electron flow to the Q_i-site, which would result in a severe decrease in bc_1 complex activity and thus in respiratory function. The thermodynamic backpressure affecting transmembrane electron transfer to b_h (or proton uptake at the Q_i-site [12]) would be released on addition of an uncoupler (such as CCCP) or in broken mitochondrial membrane preparations.

Delay in protonation of the semiquinone anion would make the second electron transfer from heme b_h energetically unfavourable [13]. This would be expected to result in ROS production due to the accumulation of electrons on the low potential chain within

cytochrome *b* and increased occupancy of semiquinone in the Q_o-site, as observed in the mutant cells (Fig.4). The redox potential of the quinone/semiquinone couple in the Q_i-site might be changed due to minor structural perturbation of the substrate binding site, altering the equilibrium constant for electron transfer from ferroheme b_h and favouring electron accumulation in the low potential chain within cytochrome *b*. Similarly, the redox potential of heme b_h could also be altered by the mutations although residues F225/K228 are quite far from heme b_h (8 Å closest approach), as has been observed in mutants of the *Rhodobacter sphaeroides* bc_1 complex [14]. We note that the redox potential of b_h is in itself likely to vary during the reaction cycle in the Q_i-site by around +100 mV on the basis of semiquinone occupancy and proximity, and that this phenomenon may be affected by mutations altering the local fold and protein environment at Q_i [12,14,15].

It may also be suggested that the F255L-K228L mutations change the distribution of Q_i-bound water (and/or the *p*Ka values of nearby proton carriers, which may include phospholipid), introducing a kinetic barrier for reduction and protonation of semiquinone [16-19]. In the suppressors, respiratory function is restored by either replacing the leucine at position 225 by the original phenylalanine, by replacing the leucine at position 228 by a methionine or by introducing changes in other residues, namely Y28, N31 or T232. The amino-acid substitutions may restore the proper water molecule (or general proton transfer) network for efficient redox chemistry at Q_i. However a solely kinetic problem is unlikely to explain the rescue of the bc_1 complex activity by CCCP and broken (uncoupled) mitochondrial membrane preparations. Thermodynamic factors arising from unfavourable heme (or quinone/semiquinone) redox potentials due to the introduced residues are also likely to play an important role in the diagnosis of these mutants.

Acknowledgements

This work was in part funded by the CNRS and Chemical Sciences, Geosciences and Biosciences Division, Office of Basic Energy Sciences, Office of Science, U.S. Department of Energy (award number DE-FG02-91ER20021).

References

[1] C. Hunte, H. Palsdottir, B.L. Trumpower, Protonmotive pathways and mechanisms in the cytochrome bc_1 complex, FEBS Lett. 545 (2003) 39–46. doi:10.1016/S0014-5793(03)00391-0.

[2] P.A. Postila, K. Kaszuba, P. Kuleta, I. Vattulainen, M. Sarewicz, A. Osyczka, T. Róg, Atomistic determinants of co-enzyme Q reduction at the Q_i-site of the cytochrome bc_1 complex, Sci. Rep. 6 (2016) 1–10. doi:10.1038/srep33607.

[3] P. Kuleta, M. Sarewicz, P. Postila, T. Róg, A. Osyczka, Identifying involvement of Lys251/Asp252 pair in electron transfer and associated proton transfer at the quinone reduction site of *Rhodobacter capsulatus* cytochrome bc_1, Biochim. Biophys. Acta - Bioenerg. 1857 (2016) 1661–1668. doi:10.1016/j.bbabio.2016.07.003.

[4] P. Mounkoro, T. Michel, R. Benhachemi, G. Surpateanu, B.I. Iorga, N. Fisher, B.

Meunier, Mitochondrial complex III Q_i-site inhibitor resistance mutations found in laboratory selected mutants and field isolates, Pest Manag. Sci. 75 (2019) 2107-2114. doi:10.1002/ps.5264.

[5] P. Hill, J. Kessl, N. Fisher, S. Meshnick, B.L. Trumpower, B. Meunier, Recapitulation in *Saccharomyces cerevisiae* of cytochrome *b* mutations conferring resistance to atovaquone in *Pneumocystis jiroveci*, Antimicrob. Agents Chemother. 47 (2003) 2725–2731. doi:10.1128/AAC.47.9.2725.

[6] N. Fisher, C.K. Castleden, I. Bourges, G. Brasseur, G. Dujardin, B. Meunier, Human disease-related mutations in cytochrome *b* studied in yeast, J. Biol. Chem. 279 (2004) 12951–8. doi:10.1074/jbc.M313866200.

[7] C. Lemaire, G. Dujardin, Preparation of respiratory chain complexes from *Saccharomyces cerevisiae* wild-type and mutant mitochondria: activity measurement and subunit composition analysis, Methods Mol. Biol. 432 (2008) 65–81. doi: 10.1007/978-1-59745-028-7_5.

[8] Z. Song, B.I. Iorga, P. Mounkoro, N. Fisher, B. Meunier, The antimalarial compound ELQ-400 is an unusual inhibitor of the bc_1 complex, targeting both Q_o and Q_i sites, FEBS Lett. 592 (2018)1346-1356. doi:10.1002/1873-3468.13035.

[9] Z. Song, J. Clain, B.I. Iorga, C. Vallières, A. Lalève, N. Fisher, B. Meunier, Interplay between the hinge region of Iron Sulfur Protein and the Q_o site in the bc_1 complex – Analysis of *Plasmodium*-like mutations in the yeast enzyme, Biochim. Biophys. Acta - Bioenerg. 1847 (2015) 1487–1494. doi:10.1016/j.bbabio.2015.08.005.

[10] L. Bleier, S. Dröse, Superoxide generation by complex III: from mechanistic rationales to functional consequences, Biochim. Biophys. Acta. 1827 (2013) 1320–31. doi:10.1016/j.bbabio.2012.12.002.

[11] A.R. Crofts, B. Barquera, R.B. Gennis, R. Kuras, M. Guergova-kuras, E.A. Berry, Mechanism of ubiquinol oxidation by the bc_1 complex : Different domains of the quinol binding pocket and their role in the mechanism and binding of inhibitors, Biochemistry 38 (1999) 15807–15826. doi:10.1021/bi990962m

[12] P.R. Rich, A.E. Jeal, S.A. Madgwick, A.J. Moody, Inhibitor effects on redox-linked protonations of the *b* haems of the mitochondrial bc_1 complex, Biochim. Biophys. Acta - Bioenerg. 1018 (1990) 29–40. doi:10.1016/0005-2728(90)90106-E.

[13] P.R. Rich, Electron and proton transfers through quinones and cytochrome *bc* complexes, Biochim. Biophys. Acta-Bioenerg. 768 (1984) 53–79. doi:10.1016/0304-4173(84)90007-7.

[14] B. Hacker, B. Barquera, A.R. Crofts, R.B. Gennis, Characterization of mutations in the cytochrome *b* subunit of the bc_1 complex of *Rhodobacter sphaeroides* that affect the quinone reductase site (Q_c), Biochemistry 32 (1993) 4403–4410. doi:10.1021/bi00067a033.

[15] A.R. Crofts, The cytochrome bc_1 complex: Function in the context of structure, Annu. Rev. Physiol. 66 (2004) 689–733. doi:10.1146/annurev.physiol.66.032102.150251.

[16] E. A. Berry, L.S. Huang, Z. Zhang, S.H. Kim, Structure of the avian mitochondrial cytochrome bc_1 complex, J. Bioenerg. Biomembr. 31 (1999) 177–90. doi:10.1023/a:1005459426843

[17] X. Gao, X. Wen, L. Esser, B. Quinn, L. Yu, C.-A. Yu, D. Xia, Structural basis for the quinone reduction in the bc_1 complex: a comparative analysis of crystal structures of mitochondrial cytochrome bc_1 with bound substrate and inhibitors at the Q_i site., Biochemistry 42 (2003) 9067–80. doi:10.1021/bi0341814.

[18] C. Lange, J.H. Nett, B.L. Trumpower, C. Hunte, Specific roles of protein-phospholipid interactions in the yeast cytochrome bc_1 complex structure, EMBO J. 20 (2001) 6591–6600. doi:10.1093/emboj/20.23.6591.

[19] C. Hunte, J. Koepke, C. Lange, T. Roßmanith, H. Michel, Structure at 2.3 Å resolution of the cytochrome bc_1 complex from the yeast *Saccharomyces cerevisiae* co-crystallized with an antibody Fv fragment, Structure 8 (2000) 669–684. doi:10.1016/S0969-2126(00)00152-0.

Legends to figures

Fig.1 Location of the mutated residues in the Q_i domain of the bc_1 complex. Cytochrome *b* is shown as a ribbon and water molecules as black dots. UQ, Ubiquinone; CDL, Cardiolipin. The figure was drawn using the structure PDB : 1KB9. The residues mutated in PFQi11 and the suppressors are shown.

Fig.2 Growth competence of WT and mutants. Cell suspensions were spotted on YDP and YPG medium and incubated for two days (YPD) or three days (YPG).

Fig.3 Oxygen consumption rates of WT and mutant cells, and effect of uncoupler. Oxygen consumption rate were measured as described in Materials and Methods with and without the uncoupler CCCP. The measurements of WT, PFQi11 and the double mutant F225L-K228L (FL-KL) have been repeated seven times and with cells from three different cultures; the measurements with the other strains were repeated three times. Valued were averaged. The error bars represent standard deviations. A) Oxygen consumption rates (mM O_2 per min per OD_{600nm} cells) without CCCP; B) Fold changes between oxygen consumption rates with and without CCCP.

Fig.4 Activity of the ROS-sensitive aconitase in WT and mutant cells. Aconitase and fumarase activities were assessed spectrophotometrically as described in Materials and Methods. The data are presented as the ratio of the aconitase activity and the fumarase activity. Values are the averages of four-five independent experiments, with error bars representing standard deviation.

Table 1 bc_1 complex activity in WT and mutants

strain	mutations	k_{cat} (s^{-1})	K_M (μM)
WT		53 +/- 2	3
F225L-K228L	F225L, K228L	28 +/- 2	7
PFQi11	M221F, F225L, K228L,V233F	48 +/- 2	7
SUP1	M221F, F225L, K228L, **T232I**, V233F	50 +/- 6	4
SUP2	**N31D**, M221F, F225L, K228L,V233F	27 +/- 3	4
SUP3	**Y28S**, M221F, F225L, K228L,V233F	43 +/- 2	4
SUP5	M221F, F225L, **K228M,**V233F	40 +/- 2	5
SUP6	M221F, **F225**, K228L,V233F	55 +/- 4	3

bc_1 complex activities were determined by measuring the reduction of cytochrome *c* using broken mitochondria. k_{cat} are cytochrome *c* reduction rates per bc_1 complex. K_M were estimated from the plots of cytochrome *c* reduction rates *vs* decylubiquinol concentrations, as the decylubiquinol concentrations required to obtain 50% of the observed maximum rate of cytochrome *c* reduction

Figure 1

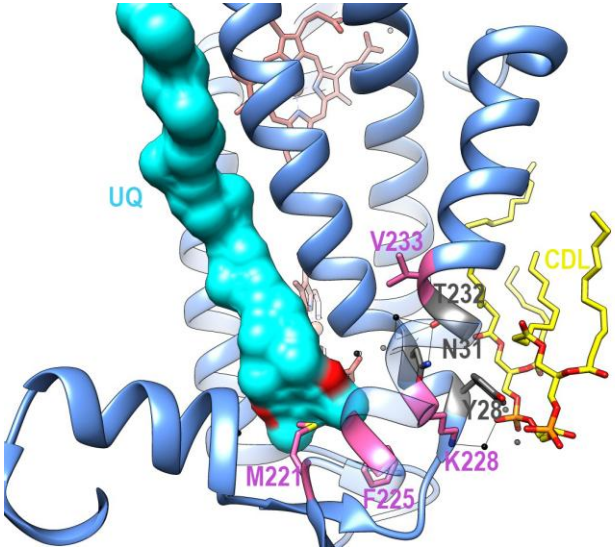

Figure 2

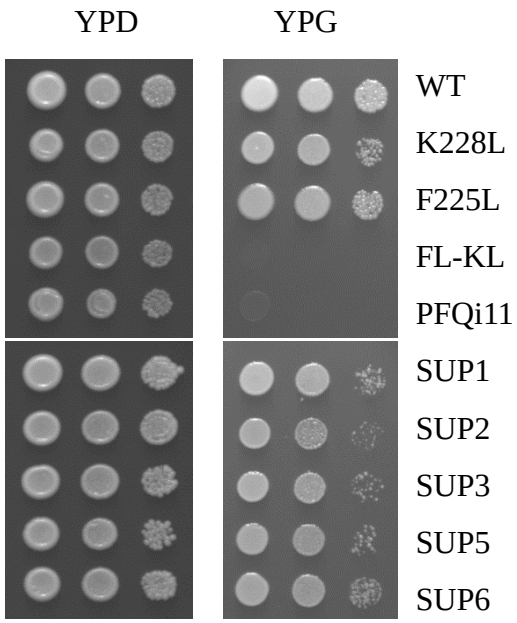

Figure 3

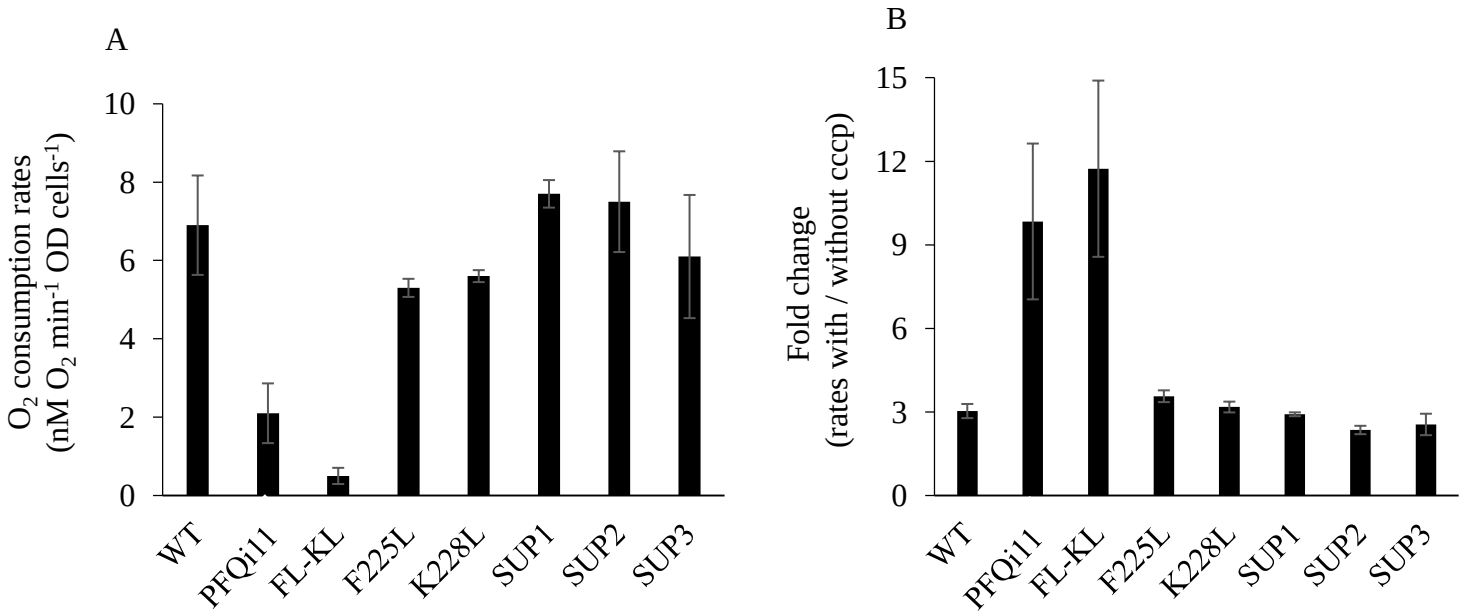
A
O_2 consumption rates
(nM O_2 min^{-1} OD $cells^{-1}$)
0
2
4
6
8
10
WT
PFQi11
FL-KL
F225L
K228L
SUP1
SUP2
SUP3
B
Fold change
(rates with / without cccp)
0
3
6
9
12
15
WT
PFQi11
FL-KL
F225L
K228L
SUP1
SUP2
SUP3

Figure 4